Collision-Assisted Spectroscopy of HCN above the Isomerization Barrier

Daniel Lessen, J. Spencer Baskin, Christopher M. Jones, Tian He, and Edwin Carrasquillo-Molina*

Department of Chemistry, University of Houston, Houston, Texas 72204-5003

Received: April 29, 2002; In Final Form: January 7, 2003

Double-resonance spectroscopy, using collisional energy transfer to populate high-lying vibrational states, reveals the location of 27 previously undetected levels in the ground electronic state of HCN. Three laser-pumped overtones, $(0,0^0,4)$, $(0,0^0,5)$, and $(1,0^0,5)$ provide the doorway through which to collisionally populate vibrational levels lying between 10330 and 17650 cm^{-1}. This greatly increases the energy range over previous studies using collision-assisted spectroscopy and provides access to states which have internal energy above the predicted isomerization barrier. Levels populated by collisions from $(0,0^0,4)$ and $(0,0^0,5)$ are detected directly via $\tilde{A}$ state fluorescence, while those from $(1,0^0,5)$ are detected through resonant multiphoton dissociation resulting in CN ($B\rightarrow X$) fluorescence. Although potentially, collision-assisted spectroscopy above the isomerization barrier could access HNC localized states, such states have not been identified in the present experiments.

I. Introduction

The relatively small size, light atoms, and stiffness of hydrogen cyanide makes this molecule a particularly good model system for high-energy and chemical dynamics investigations. Portions of its ground-state potential surface have been well characterized by numerous theoretical[1−10] and experimental investigations.[11−19] Of considerable interest is the accurate description of the global potential surface for HCN/HNC isomerization. Toward this end, more spectroscopic data in the region near the isomerization barrier is important. For instance, while ab initio calculations place this barrier at 16733 cm^{-1} above the absolute minimum of the potential,[7] direct experimental evidence has yet to be obtained.

The majority of experimental contributions to the spectroscopy of HCN at very high vibrational excitation come from two complementary techniques: direct overtone absorption[14−17] and stimulated emission pumping (SEP).[11,12] In the absence of perturbations, direct overtone absorption studies mainly uncover states built on vibrational progressions that possess large anharmonicity, for instance, those built on the CH stretch. SEP studies, on the other hand, involve transitions to and from the bent $\tilde{A}$ state of HCN. Consequently, they preferentially access ground-state levels with high excitation in the bending mode because of favorable Franck Condon factors. The earlier two-color SEP studies of Wodtke et al. are particularly interesting because of the characterization of vibrational levels possessing up to 14 quanta in the bend and because the minimum energy path for HCN−HNC isomerization occurs through high-bending excitation. The asset but also a weakness of the latter SEP experiments is their selectivity. For instance, many states remain undiscovered because of the strong propensity rules that govern the direct laser excitation method.

The work presented here utilizes a different approach, collision-assisted spectroscopy (CAS), which is made possible by the success of experiments in resolving the collision-induced vibrational state-to-state relaxation at high excitation.[20] It attests to the ability of this technique to probe vibrational levels having internal energy above the isomerization barrier. The CAS approach is a double-resonance method which also uses the $\tilde{A}$ state of HCN, complementing the above spectroscopic techniques. Here, collisional energy transfer from a laser-pumped overtone vibration populates other levels which may be probed by laser-induced fluorescence via the $\tilde{A}$ state. Investigation of different energy regions of the ground-state potential surface can be accomplished by varying the overtone state initially prepared. The CAS approach accesses a variety of undiscovered states. For instance, it readily discerns vibrational levels containing odd quanta in the bend as well as detecting states with excitation in all three modes, which was difficult in the previous SEP experiments.[11,12] We report in this study the location of states collisionally populated from three initially prepared levels: $(0,0^0,4)$: $E_{vib} = 12635.888$ cm^{-1}, $(0,0^0,5)$: $E_{vib} = 15551.944$ cm^{-1}, and $(1,0^0,5)$: $E_{vib} = 17550.42$ cm^{-1}. In the latter, the vibrational state labeling corresponds to v_1, v_2, v_3 where v_1 is the CN stretch, v_2 is the bending mode, v_3 is the CH stretch, and l refers to the vibrational angular momentum.

Earlier studies carried out at lower energy content showed the success of the CAS approach.[18,19,21] They resolved the vibrational structure of HCN in the ground electronic state and also explored the spectroscopy of the first excited electronic state via probe excitation from collisionally populated levels. This work demonstrates that the CAS approach can be applied to the very high energy regions. It was made possible at the higher excitation by probing HCN via photodissociation with subsequent detection of CN emission rather than by monitoring the HCN laser-induced fluorescence as carried out at lower energies.

II. Experimental Section

At the center of these studies is the population of previously undetected states of highly excited hydrogen cyanide by collision-induced relaxation from a laser-pumped overtone vibration. The experiments were carried out in a cell filled with

* To whom correspondence should be addressed. E-mail: Mcarrasquillo@uh.edu.

10.1021/jp021075n CCC: $25.00
Published on Web 07/03/2003

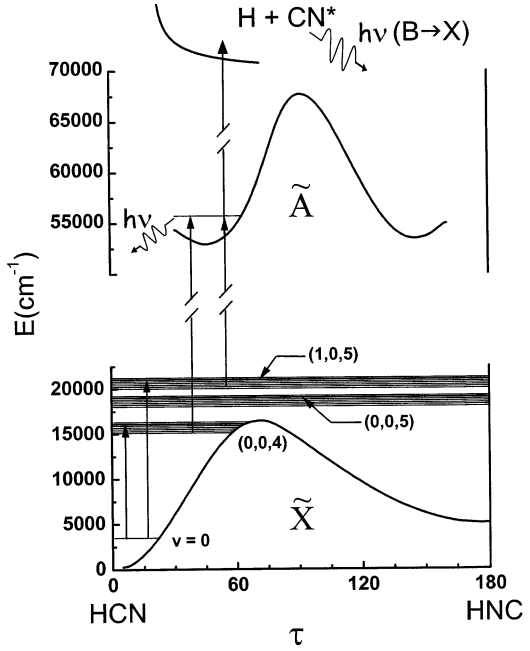

Figure 1. Laser excitation scheme utilized in the experiments. The potentials are adapted from ref 9 and represent the minimum energy path. The vibrational levels do not necessarily span both wells.

neat HCN gas—see below. After several collisions, adjustable by controlling the cell pressure and the pump-to-probe time delay, a variety of vibrational levels are populated. These levels, which would not be easily detected by direct-absorption methods, were then probed through a fluorescing level of the $\tilde{A}$ state or via the fluorescence obtained by photodissociation from the $\tilde{A}$ state as shown in Figure 1.

As depicted in Figure 1, the overall laser excitation scheme for the preparation and detection of highly vibrationally energized hydrogen cyanide consisted of a two-color, double-resonance procedure. First, a Continuum 581C Nd^{3+}:YAG/TDL50A dye laser system provided the pump laser which initially prepared a small fraction of the HCN molecules in a selected high-lying vibrational state by exciting an overtone transition that is known to absorb. For this study, the $\tilde{X}(1,0^0,5) \leftarrow \tilde{X}(0,0^0,0)$ and the $\tilde{X}(0,0^0,5) \leftarrow \tilde{X}(0,0^0,0)$ transitions were pumped directly using conventional dyes, R6G and DCM, respectively. To populate $(0,0^0,4)$, the first stokes of the DCM output was Raman-shifted in methane. The optimized laser output powers for preparing the $(0,0^0,4)$, $(0,0^0,5)$, and $(1,0^0,5)$ states were 4.5, 55, and 67 mJ/pulse, respectively. To tune the pump laser wavelength on the $(0,0^0,4)$ transition, the laser beam was directed through a photoacoustic cell filled with 50 Torr of HCN and the signal was monitored. The photoacoustic method, however, was not possible for the $(0,0^0,5)$ and $(1,0^0,5)$ transitions because of the much smaller overtone absorption cross sections. For these transitions, we made use of the fact that collisions efficiently populate the $(2,4^0,0)$ level (E_{vib} = 6951.68 cm^{-1}), as shown by our previous studies at lower energy content,[21] and optimized the pump laser wavelength by taking double-resonance action spectra instead. Here, the probe laser was fixed on a well-characterized $\tilde{A} \leftarrow \tilde{X}$ transition from the collisionally populated $(2,4^0,0)$ $\tilde{X}$ state level and the resultant fluorescence was monitored as the pump laser was tuned to excite the $(0,0^0,5)$ or $(1,0^0,5)$ overtone states.

The laser for the probe step consisted of an excimer pumped dye laser system (Questek 2520 vβ/ FL 3002 CES) whose output was frequency doubled in BBO, leading to 500−700 μJ/pulse over the wavelength region investigated. The dyes utilized in the probe step were Exalite 428, Coumarin 480, Coumarin 500, Coumarin 540, and Fluorescein 548 providing wavelength coverage between 210 and 217 nm and 233−289 nm after frequency doubling. The lower wavelength range merely probed known states such as $(2,4^0,0)$ which were previously characterized but in studies at lower energy content.[18,19,21] Separation of the frequency doubled output from the visible fundamental was accomplished with a set of four S1UV Pellin Brocca prisms or above 510 nm with a $NiSO_4/CoSO_4$ liquid filter solution.

The pump and probe laser beams counterpropagated at time delays between 0 and 2 μs through a cylindrical laser-induced fluorescence cell made of Pyrex but equipped with S1UV windows. The fluorescence cell contained neat HCN gas at a pressure of 1−4 Torr. Both lasers were focused at the center of the cell and the resultant fluorescence collected from the center of the cell normal to the laser axis were passed through wavelength filters as outlined below and imaged onto an EMI 9813QB photomultipler tube. The output of the photomultiplier tube was subsequently integrated with a gated LeCroy 2249SG analogue to digital converter which was interfaced through a Camac crate to a lab computer. Collisionally populated states in the lower energy region were detected by collecting laser-induced fluorescence from low-lying levels of the $\tilde{A}^1A''$ electronic state. However, for vibrational energies roughly above 12000 cm^{-1}, fluorescence intensities were too low, necessitating a new approach. Above this energy range, experiments were made possible by monitoring the CN fragment fluorescence induced by two-photon resonant-enhanced photodissociation via the $\tilde{A}$ state. Fluence dependence studies confirm that the probe step is a two-photon process, the first photon being resonant with a low-lying level of the $\tilde{A}$ state and the second accessing a dissociative state (probably the $\tilde{C}$ or $\tilde{D}$ state[22−24]). The experiments revealed that significantly more signal could be obtained by monitoring the CN B → X emission than by collecting the HCN $\tilde{A}$ state fluorescence. Using various fluorescence filters and filter combinations, it was determined that the majority of emission from the photodissociation was from the B → X (0,0) transition. Depending on the probe laser wavelength region and detection scheme used, the best results were obtained when the fluorescence, on its way to the photomultiplier tube, was first passed through either a Janos 220 nm interference filter, a Janos 250 nm interference filter, a Schott UG1 filter, or a combination Schott WG335, Schott BG3, and CVI 400 nm interference filter. Figure 1 displays the two pump−probe configurations utilized in this study for preparing and detecting highly excited vibrational levels of HCN.

The emphasis of this work is on the analysis of states collisionally populated after initially preparing HCN molecules in the $J = 8$ level of $(1,0^0,5)$. Data were calibrated with the well-known I_2 transitions for visible probe laser wavelengths greater than 5513 Å. Bandhead assignments were not calibrated directly in the $(0,0^0,4)$ and $(0,0^0,5)$ experiments and are estimated to ± 2 cm^{-1}. Further details of the experimental apparatus and procedure may be found in the literature.[18,19,21]

III. Results

Accessing vibrational states high in the potential surface becomes increasingly difficult because of the decreasing absorption cross section of a given overtone. Nonetheless, the desire to understand the HCN−HNC isomerization stimulates interest in characterizing the spectroscopy and molecular behavior at vibrational energies sufficient to isomerize. This study extends previous investigations using collision-assisted spectroscopy below 12000 cm^{-1} to energies up to 17650 cm^{-1} above the

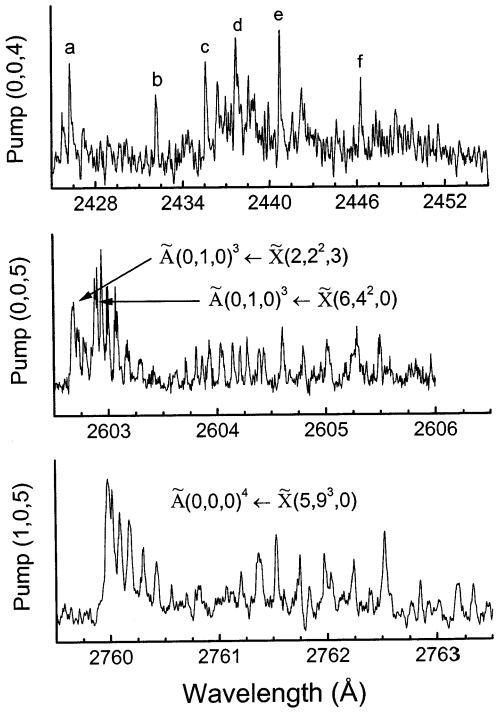

Figure 2. Laser-induced fluorescence spectra obtained by initially preparing HCN molecules in the $(0,0^0,4)$, $(0,0^0,5)$, or $(1,0^0,5)$ overtone states. The $\tilde{A} \leftarrow \tilde{X}$ transitions in the upper panel are assigned as follows: (a) $(0,1,0)^4 \leftarrow (5,3^3,0)$; (b) $(0,1,0)^2 \leftarrow (4,1^1,1)$; (c) $(0,1,0)^1 \leftarrow (3,4^0,1)$; (d) $(0,1,0)^0 \leftarrow (4,1^1,1)$; (e) $(0,1,0)^2 \leftarrow (5,3^1,0)$; and (f) $(0,1,0)^0 \leftarrow (5,3^1,0)$.

zero-point level which is ca. 4400 cm^{-1} above the predicted barrier to isomerization along the minimum energy path.[4,7] Figure 2 displays three fluorescence spectra obtained by selectively exciting the $(0,0^0,4)$ (upper), $(0,0^0,5)$ (middle), and $(1,0^0,5)$ (lower) overtone states. The latter excitation leads to HCN molecules with initial vibrational energies of approximately 12636, 15552, and 17550 cm^{-1}, respectively.

In all three cases, several previously undiscovered bands as well as several known transitions are readily observed by utilizing collisions to populate levels from the initially prepared overtone vibration. Since the emphasis of this work is on states collisionally populated from $(1,0^0,5)$, only an abbreviated examination of bands resulting from initially preparing the $(0,0^0,4)$ and $(0,0^0,5)$ overtone states were carried out. The latter studies, however, were instrumental in establishing the need for a different approach in the probe step for the higher energy investigations as was discussed in the Experimental Section. The energy regions for the $(0,0^0,4)$ and $(0,0^0,5)$ experiments could not be rigorously calibrated. Bandhead assignments are estimated to be accurate to within ± 2 cm^{-1} on the basis of comparisons with better calibrated regions.

Figure 2 illustrates representative spectra that can be obtained in the CAS experiments. The upper panel shows a coarse, broad wavelength scan revealing the bandheads of several new transitions obtained by initially preparing HCN molecules in the $(0,0^0,4)$ state. Within this region, bands arising from at least four unique ground-state levels are evident. The labeling in the $\tilde{A}$ state follows $(v_{CN},v_{bend},v_{CH})^K$ where K is the rotational angular momentum component along the near-symmetry axis of HCN. Bandheads in this work were assigned by comparison with all projected bandhead locations and contours within ± 10 cm^{-1} obtained from the known $\tilde{A}$ state constants[18,19,21] and the predicted ground-state term energies from Carter et al.[5,25] The latter were extended to other J levels and ℓ states with the rovibrational constants obtained from existing anharmonic expansions.[16,17] The presence of other $K-\ell$ sub-band transitions and that of transitions to both the (0,0,0) and (0,1,0) $\tilde{A}$ state vibrational levels provided consistency checks for the assignments. Table 1 lists all of the newly observed transitions from collisionally populated levels that were assigned in this fashion and their bandhead location.

TABLE 1: Bandhead Locations over the Region from 10330 to 17650 cm^{-1}[f]

bandhead	$G_{v,\lvert\ell\rvert}$[a]	literature[b]	predicted	transition $\tilde{A} \leftarrow \tilde{X}$
		Pump$(0,0^0,4)$		
40256.6	12199.3		12199.94	$(0,0,0)^3 \leftarrow (3,4^2,1)$
40431.4	12166.7		12168.26	$(0,0,0)^4 \leftarrow (2,7^3,1)$
	12981.9		12979.26	$(0,1,0)^3 \leftarrow (1,2^2,3)$
40572	11695.8	11696.4(20)[c,d]	11696.24	$(0,0,0)^0 \leftarrow (4,5^1,0)$
40867.5	12339.5		12340.02	$(0,1,0)^0 \leftarrow (5,3^1,0)$
40960.9	12339.8		12340.02	$(0,1,0)^2 \leftarrow (5,3^1,0)$
41011.1	12196.7		12195.53	$(0,1,0)^0 \leftarrow (4,1^1,1)$
41047.2	12184.7		12185.46	$(0,1,0)^1 \leftarrow (3,4^0,1)$
41104.6	12196.4		12195.5	$(0,1,0)^2 \leftarrow (4,1^1,1)$
41204	12365.4		12366.05	$(0,1,0)^4 \leftarrow (5,3^3,0)$
41212.4	12200.5		12199.94	$(0,1,0)^3 \leftarrow (3,4^2,1)$
41544.7	11685.4		11685.03	$(0,1,0)^1 \leftarrow (3,8^0,0)$
	11053.5		11053.00	$(0,0,0)^4 \leftarrow (3,7^3,0)$
41579	11654.8	11654.6(20)[c]	11653.83	$(0,1,0)^1 \leftarrow (5,2^0,0)$
41681.1	11525.2		11524.26	$(0,1,0)^0 \leftarrow (3,3^1,1)$
41746.9	11667.3	11667.3(20)[c]	11666.90	$(0,1,0)^3 \leftarrow (5,2^2,0)$
42015.4	10337.2		10338.04	$(0,0,0)^2 \leftarrow (4,3^1,0)$
Pump $(0,0^0,5)$				
37454.9	15000.8	15000.81(26)[e]	15002.01	$(0,0,0)^3 \leftarrow (2,2^2,3)$
37,452.0	15005.7	15004.54(12)[d]	15005.65	$(0,0,0)^3 \leftarrow (6,4^2,0)$
38032.1	14322.4		14320.23	$(0,0,0)^2 \leftarrow (6,3^1,0)$
38084.8	14371.0	14370.59(5)[c]	14370.93	$(0,0,0)^3 \leftarrow (5,6^2,0)$
38228.1	15005.0	15004.54(12)[d]	15002.01	$(0,1,0)^1 \leftarrow (6,4^2,0)$
38240.8	14992.2	14992.06(12)[d]	14992.92	$(0,1,0)^1 \leftarrow (6,4^0,0)$
38408	15005.1	15004.54(12)[d]	15005.65	$(0,1,0)^3 \leftarrow (6,4^2,0)$
38411.8	15000.9	15000.81(26)[e]	15002.01	$(0,1,0)^3 \leftarrow (2,2^2,3)$
38432.0	14798.7		14797.66	$(0,1,0)^1 \leftarrow (3,8^0,1)$
38514.4	15054.1		15052.20	$(0,1,0)^4 \leftarrow (5,7^3,0)$
38598.1	14814.2		14812.61	$(0,1,0)^3 \leftarrow (3,8^2,1)$
38722.3	15042.3		15043.88	$(0,1,0)^5 \leftarrow (6,4^4,0)$
38945.3	14354.0	14354.65(39)[d]	14354.05	$(0,1,0)^2 \leftarrow (4,9^1,0)$
38979.7	14322.1		14320.23	$(0,1,0)^2 \leftarrow (6,3^1,0)$
39224.9	14345.3		14345.36	$(0,1,0)^4 \leftarrow (6,3^3,0)$
Pump $(1,0^0,5)$				
34795.8	17660.7		17659.49	$(0,0,0)^3 \leftarrow (6,8^2,0)$
34961.2	17640.5		17642.30	$(0,0,0)^4 \leftarrow (7,5^3,0)$
35685	17615.6		17617.38	$(0,1,0)^2 \leftarrow (7,5^1,0)$
35929.2	17641.5		17642.30	$(0,1,0)^4 \leftarrow (7,5^3,0)$

[a] Estimated error is ± 2 cm^{-1}. [b] Error bars are interpreted as the equivalent of 3σ. [c] Values are from ref 12. [d] Values are from ref 11. [e] Transition from ref 11 reassigned in ref 17. [f] All quantities are in cm^{-1}.

In the middle panel, Figure 2 displays a more detailed spectrum obtained by initially preparing HCN molecules in the $(0,0^0,5)$ state. The panel shows new transitions from two closely lying levels that have been formerly characterized: $(2,2^2,3)$ and $(6,4^2,0)$.[27] Congestion of the bands complicates a fit to the spectrum; nonetheless, the vibrational term energies and rotational constants obtained are in accord with the previous measurement. This spectrum serves to illustrate how transitions from collisionally populated levels can be resolved when HCN molecules are initially prepared in the $(0,0^0,5)$ overtone state. Previously undetected vibrational levels were also revealed from this overtone state. Their band assignments and bandhead locations are additionally listed in Table 1.

Last, the bottom panel of Figure 2 displays a rotationally resolved transition from the previously unobservable $(5,9^3,0)$ level which is accessed by collision-induced population transfer from the $(1,0^0,5)$ overtone state. Calibration and rovibrational analysis of this spectrum was possible as outlined below, leading to a vibrational term energy and rotational constant of 16336.73-

TABLE 2: Comparison of HCN $\tilde{X}$ State Constants (cm^{-1})

state	$G_{v,\|l\|}$[a] this work	$B_{v,\|l\|}$[a] this work	$G_{v,\|l\|}$[b] literature	$B_{v,\|l\|}$[b] literature	observed[e] transitions
$(7,4^0,0)$	16947.9(1)	1.417(2)	16947.72(1)[c]	1.419(1)[c]	$(0,1,0)^1$
$(7,4^2,0)$	16959.33(3)	1.4163(7)	16959.22(1)[c]	1.417(2)[c]	$(0,0,0)^3$
					$(0,1,0)^3$
$(5,10^0,0)$	16984.0(5)		16983.721(57)[d]	1.4636(18)[d]	$(0,1,0)^1$
$(5,10^2,0)$	16998.2(5)		16998.072(57)[d]	1.4636(18)[d]	$(0,0,0)^3$
$(5,9^1,0)$	16338.2(5)		16338.15	1.4582	$(0,0,0)^2$
$(5,9^3,0)$	16366.73(5)	1.4566 (4)	16366.21	1.4566	$(0,0,0)^2$
					$(0,0,0)^4$
$(5,5^3,1)$	16857.86(1)	1.4342 (3)	16854.87	1.4334	$(0,0,0)^4$
$(6,7^1,0)$	16992.9(3)		16992.98	1.4392	$(0,0,0)^2$
$(6,7^3,0)$	17019.17(2)	1.4376 (1)	17019.47	1.4376	$(0,0,0)^4$
$(6,7^5,0)$	17071.85(4)	1.4336(2)	17072.54	1.4343	$(0,0,0)^4$
					$(0,0,0)^6$
$(8,2^0,0)$	17544.28(4)	1.4011 (2)	17540.95	1.4011	$(0,1,0)^3$
$(8,2^2,0)$	17553.27(4)	1.4007 (1)	17551.20	1.4003	$(0,1,0)^1$

[a] Error bars are 90% confidence limits. [b] List of experimental and predicted values. Error bars interpreted as equivalent to 3σ for experimental values. Predicted values are obtained from refs 5,16. [c] Experimental values are obtained from ref 12. [d] Experimental values are obtained from ref 11. [e] Only the upper state is listed for the $\tilde{A} \leftarrow \tilde{X}$ transition.

(5) cm^{-1} and 1.4566(4) cm^{-1}, respectively. Table 2 reports the band assignments and rovibrational constants derived by initially preparing HCN molecules in the $(1,0^0,5)$ overtone state. In all, 27 new vibrational states have been identified over the energy range between 10330 and 17650 cm^{-1}. In addition, 9 bands have been rotationally characterized.

The rotationally resolved transitions obtained by initially preparing HCN molecules in the $(1,0^0,5)$ overtone state were calibrated with the well-known I_2 visible lines. Rotational analysis was performed using eq 1 and correcting for ℓ-type resonance.

$$E(v,J,\ell) = G_{v,|\ell|} + B_{v,|\ell|}J(J+1) - D_{v,|\ell|}[J(J+1) - \ell^2]^2 \quad (1)$$

Here, $G_{v,|\ell|}$ refers to the vibrational term energy. $B_{v,|\ell|}$ and $D_{v,|\ell|}$ are the rotational and centrifugal distortion constants, respectively. In all rotationally resolved cases, $G_{v,|\ell|}$ and $B_{v,|\ell|}$ were fit to observed vibronic transitions with a nonlinear least-squares program based on the Levenberg−Marquardt algorithm. Parameters for the $\tilde{A}$ state are given in the bibliography.[18,19,21] Since the spectroscopic data was not sufficient to independently establish the centrifugal distortion constant, fits for a given band were performed with a projected value based on published anharmonic expansions.[16,17] The effect of ℓ-type resonance is included in all rotational fits by diagonalizing the **e** and **f** matrixes as outlined in the literature.[17] For n_2 even, the ℓ-type resonance constant, q, is determined from the predictions of the empirical force field of Carter et al.[5] while for ν_2 odd, the equilibrium value of q is used, for example, 7.27×10^{-6} cm^{-1}. The zero-order energies, for example, the diagonal elements of the **e** and **f** matrixes needed for determining the magnitude of the ℓ-type resonance, are obtained from eq 1 with the observed data or from the semiempirical predictions of Carter et al. extended, as necessary, with the aid of present anharmonic expansions.[16,17]

As final examples, Figures 3 and 4 display the fluorescence excitation spectrum of the $\tilde{A}(0,1,0)^3 \leftarrow \tilde{X}(8,2^2,0)$, $\tilde{A}(0,0,0)^4 \leftarrow \tilde{X}(6,7^3,0)$, and $\tilde{A}(0,0,0)^4 \leftarrow \tilde{X}(5,5^3,1)$ transitions and their rotational assignment. These transitions were derived by initially preparing HCN molecules in the $(1,0^0,5)$ overtone state. They were assigned by considering the possible transitions within ± 10 cm^{-1}. The band contour, intensity profile, and consistency of spectroscopic parameters with those predicted by theory,[5,16,17] all indicate we have the correct assignment. For the $(8,2^2,0)$ band, further evidence is provided by the low fluorescence intensity of the Q(10) transition which has previously been observed as characteristic of the $K = 3$ level of the $\tilde{A}(0,1,0)$ vibrational state.[21]

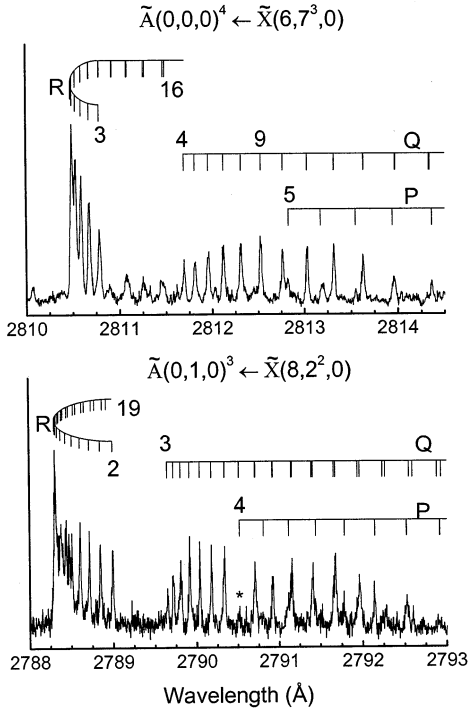

Figure 3. Rotationally resolved transitions obtained by initially preparing HCN molecules in the $(1,0^0,5)$ overtone state.

In all, for the $(1,0^0,5)$ experiments, complete rotational analysis of six previously undetermined states has been performed and the results tabulated in Table 2. With the aid of Carter et al.'s predictions,[5] two additional bands of different ℓ components ($(5,9^10)$ and $(6,7^10)$) have also been identified. Although the spectra for the latter was not of sufficient quality to perform a complete rotational analysis, band origins can be estimated on the basis of fitting the rotational profile with predicted rotational constants.[16,17] The vibrational term energies so derived have also been included in Table 2.

IV. Discussion

Spectroscopic studies in the energy regime near the barrier to isomerization are important, as for instance, the location and nature of the vibrational state can play a critical role in tunneling

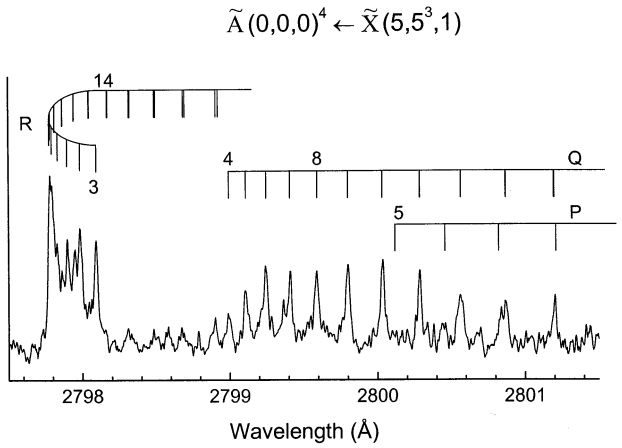

Figure 4. Rotationally resolved transition obtained by initially preparing HCN molecules in the $(1,0^0,5)$ overtone state.

just below the barrier.[28] This work shows that collision-assisted spectroscopy can be extended to investigate HCN molecules from below the barrier up to energies above the barrier to isomerization. At the higher energy regime, a different approach is much more effective in the probe step. It consists of monitoring the CN fragment emission induced by two photon dissociation via the $\tilde{A}$ state of HCN.

Several states in the energy range between 10330 cm^{-1} and 17650 cm^{-1} were detected by initially preparing HCN molecules in the $(0,0^0,4)$, $(0,0^0,5)$, and $(1,0^0,5)$ overtone states. These newly accessible levels were identified and their vibrational term energies were derived either via their bandhead assignments or, in the $(1,0^0,5)$ experiments where calibration was possible, via their rotationally resolved spectra. Of particular interest is that by utilizing collisions to carry out the spectroscopic studies, higher ℓ states could be detected than can typically be accomplished with the overtone absorption or SEP methods; odd-bending states could be readily discerned which was difficult in the previous SEP studies, and levels with up to 10 quanta in the bend could be resolved. In addition, some states with excitation in all three modes could be observed. The new data should help improve the current global potential energy surface (PES) of HCN/ HNC which was recently refined significantly by adjustment of the ab initio results via a singular value decomposition method to match the experimentally observed vibrational structure.[8] The potential for improving the PES is especially evident for states with excitation in all three modes which systematically show the greatest deviation from the predictions of the semiempirical global surface.[8]

An obvious question is whether CAS via self-relaxation can access HNC states. The current picture obtained by theoretical projections of collision-induced isomerization with Ar is that collisions first populate delocalized levels from HCN localized states and then relax these delocalized levels into HNC localized states.[29,30] The delocalized states can be accessed via high-bend excitation. Self-relaxation, for example, mostly in collisions with vibrationless HCN molecules because of the low efficiency of overtone vibration excitation, should facilitate large quantum changes for the energized molecules because of the permanent dipole moment of HCN. Indeed, this has been shown previously in state-to-state collisional relaxation studies.[20,31] Population transfer between weakly coupled states, such as the 2:3 CH to CN resonance,[32] the 1:3 CN to bend resonance,[17] and the 1:1 CH to CN resonance appearing at high energy[33] could, as shown in at least one case for HCN,[20] be enhanced in collisions with other HCN molecules. These expectations are consistent with the fact that the states populated and detected in the present experiments involve the exchange of many CH quanta for bending and CN stretching quanta. Even though there exists no experimental observation of the HNC $\tilde{A}$ state or of high-lying $\tilde{X}$-state vibrational levels, current theory indicates that the HNC vibrational states at the energy of the experiments should give rise to some of the stronger HNC $\tilde{A} \leftarrow \tilde{X}$ transitions.[9] Nonetheless, no clear evidence of HNC levels have yet been identified. This is likely because the reaction coordinate for isomerization basically corresponds to the bend. The regular nature observed for the vibrational structure of HCN indicates weak coupling at best to this coordinate, leading to the expectation that vibrational energy about 16000 cm^{-1} should appear in the bend to reach the threshold for isomerization. The latter is supported by the perturbation calculations of Sugny et al.[28] on the basis of the ab initio surface of Bowman and co-workers[4] and carried out assuming decoupled bending and stretching states. They calculate that the $(1,0^0,5)$ level lies 1800 cm^{-1} above the barrier to isomerization of pure bending states, 158 cm^{-1} below that to isomerization via bending excitation of states possessing one quanta in the CN stretch but none in CH, and well below the barrier to isomerization of any other stretching state. Consequently, on energetic grounds, it appears that collisions can access only a few states from $(1,0^0,5)$ that can isomerize and they possess a very high number of quanta in the bend. In addition, no clear evidence of the delocalized states has been found. The latter is not surprising since the Franck−Condon factors for these states are expected to be much weaker than for the localized ones.[4] It is possible that HNC states could be discovered by collision-assisted spectroscopy based on self-relaxation. The best opportunities appear to be at even higher excitation energies. The capability of CAS to probe higher excitation energies is currently under investigation.

V. Summary

This work shows that collision-assisted spectroscopy can be extended to probe the HCN vibrational structure up to energies above the barrier to isomerization. With this technique, the term energies and rotational constants for six previously unobserved vibrational states have been determined. Also, bandhead assignments for an additional 31 new transitions in the region 10330 to 17650 cm^{-1} have been possible. Collision-assisted spectroscopy complements other spectroscopic techniques involving direct laser excitation and could potentially probe HNC localized states via collision-induced isomerization.

Acknowledgment. The financial support of the Robert A. Welch Foundation of Texas and the Advanced Research Program of the Texas Higher Education Coordinating Board for this research is gratefully acknowledged.

References and Notes

(1) Lang, B. L.; Bowman, J. M. *J. Phys. Chem.* **1993**, *97*, 12535.
(2) McCoy, A. B.; Sibert, E. L., III. *J. Chem. Phys.* **1991**, *95*, 3476.
(3) Bentley, J. A.; Huang, C. M.; Wyatt, R. E. *J. Chem. Phys.* **1993**, *98*, 5207.
(4) Bowman, J. M.; Gazdy, B.; Bentley, J. A.; Lee,T. J.; Dateo, C. E. *J. Chem. Phys*. **1993**, *99*, 308.
(5) Carter, S.; Mills, I. M.; Handy, N. C. *J. Chem. Phys*. **1993**, *99*, 4379.
(6) Wong, A. T.; Bacskay, G. B. *Mol. Phys.* **1993** *79*, 819.
(7) van Mourik, T.; Harris, G. J.; Polyansky, O. L.; Tennyson, J.; Császár; A. G.; Knowles, P. J. *J. Chem. Phys.* **2001**, *115*, 3706.
(8) Wu, Q.; Zhang, J. Z. H.; Bowman, J. M. *J. Chem. Phys.* **1997**, *107*, 3602.
(9) Gazdy, B.; Musaev, D. G.; Bowman, J. M.; Morokuma, K. *Chem. Phys. Lett.* **1995**, *237*, 27.

(10) Bowman, J. M.; Irle, S.; Morokuma, K.; Wodtke, A. *J. Chem. Phys.* **2001**, *114*, 7923.
(11) Jonas, D. M.; Yang, X. M.; Wodtke, A. M. *J. Chem. Phys.* **1992**, *97*, 2284.
(12) Yang, X. M.; Rogaski, C. A.; Wodtke, A. M. *J. Opt. Soc. Am. B* **1990**, *7*, 1835.
(13) Yang, X. M.; Rogaski, C. A.; Wodtke, A. M. *J. Chem. Phys.* **1990**, *92*, 2111.
(14) Quapp, W.; Klee, S.; Mellau, G. C.; Albert, S.; Maki, A. *J. Mol. Spectrosc.* **1994**, *167*, 375.
(15) (a) Romanini, D.; Lehmann, K. K. *J. Chem. Phys.* **1993**, *99*, 6287. (b) Romanini, D.; Lehmann, K. K. *J. Chem. Phys.* **1995**, *102*, 633. (c) Romanini, D.; Lehmann, K. K. *J. Chem. Phys.* **1996**, *105*, 68.
(16) Smith, A. M.; Coy, S. L.; Klemperer, W.; Lehmann, K. K. *J. Mol. Spectrosc.* **1989**, *134*, 134.
(17) Maki, A.; Quapp, W.; Klee, S.; Mellau, G. C.; Albert, S. *J. Mol. Spectrosc.* **1996**, *180*, 323.
(18) Baskin, J. S.; Saury, A.; Carrasquillo, M. E. *Chem. Phys. Lett.* **1993**, *214*, 257.
(19) Saury, A.; Wu, J.; Carrasquillo, M. E. *J. Mol. Spectrosc.* **1994**, *164*, 416.
(20) Huang, R.; Wu, J.; Gong, M.; Saury, A.; Carrasquillo, M. E. *Chem. Phys. Lett*. **1993**, *216*, 115.
(21) Saury, A. Ph.D. Thesis, University of Houston, 1995.
(22) Cock, P. A.; Langford, S. R.; Ashfold, M. N. R.; Dixon, R. N. *J. Chem. Phys.* **2000**, *113*, 994.
(23) Morley, G. P.; Lambert, I. R.; Ashfold, M. N. R.; Rosser, K. N.; Western, C. M. *J. Chem. Phys.* **1992**, *97*, 3157.
(24) Guo, J.; Eng, R.; Carrington, T.; Filseth, S. V. *J. Chem. Phys.* **2000**, *112*, 8904.
(25) Although not a global surface, considerable amount of data (see refs 17, 21, 26) now indicate a high degree of success for the empirical force field of ref 5 in predicting localized HCN ground-state energies.
(26) Romanini, D.; Lehmann, K. K. *J. Chem. Phys.* **1996**, *105*, 81.
(27) Transitions in ref 11 were reassigned in ref 17.
(28) Sugny, D.; Joyeux, M.; Sibert, E. L., III. *J. Chem. Phys.* **2000**, *113*, 7165.
(29) Christoffel, K. M.; Bowman, J. M. *J. Chem. Phys.* **2000**, *112*, 4496.
(30) Bowman, J. M.; Gazdy, B. *J. Phys. Chem. A* **1997**, *101*, 6384.
(31) Huang, R.; Wu, J.; Gong, M.; Saury, A.; Carrasquillo. M. E. *Chem. Phys. Lett.* **1993**, *216*, 108.
(32) Allen, H. C., Jr.; Tidwell, E. D.; Plyler, E. K. *J. Chem. Phys.* **1956**, *25*, 302.
(33) Lehmann, K. K. *Mol. Phys.* **1989**, *66*, 1129; *erratum* **1992**, *75*, 739.